Agricultural and Forest Meteorology 323 (2022) 109082

Contents lists available at ScienceDirect

Agricultural and Forest Meteorology

journal homepage: www.elsevier.com/locate/agrformet

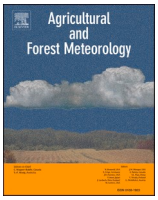

Disparate response to water limitation for vessel area and secondary growth along *Fagus sylvatica* southwestern distribution range

JM Olano [a,*], H Hernández-Alonso [a,b], G Sangüesa-Barreda [a], V Rozas [a], AI García-Cervigón [c], M García-Hidalgo [a]

[a] *iuFOR-EiFAB, Campus de Soria, Universidad de Valladolid, Soria E-42004, Spain*
[b] *Area of Ecology, Faculty of Biology, University of Salamanca, Salamanca E-37007, Spain*
[c] *Biodiversity and Conservation Area, Rey Juan Carlos University, c/Tulipán s/n, Móstoles E-28933, Spain*

ARTICLE INFO

Keywords:
Climate
Fagus sylvatica
Marginal populations
Quantitative wood anatomy
Secondary growth
Tree rings

ABSTRACT

The response of European beech (*Fagus sylvatica* L.) to climate warming will depend on the ability of their populations to adjust tree performance to water shortage. By exploring inter- and intra-annual variations in secondary growth and mean vessel area (MVA), we assessed the effects of precipitation on cambial activity and hydraulic control during the vessel expansion phase along tree lifes. We sampled beech populations at low and high altitude from four mountain ranges across its southwestern distribution edge. We measured a total of 45,897 rings from 126 trees and 5.5 million vessels from 76 trees. We built chronologies for ring width and MVA between 1950 and 2017, calculated their climate responses and evaluated the effects of region, altitude and chronology type (ring-width vs. MVA) by means of ordinations (PCA) and constrained ordinations (pRDA). Precipitation controlled ring width and MVA along beech's southwestern distribution range, but at different time domains. Ring width responded primarily to summer precipitation during the previous growing season, whereas MVA responded to water availability during the vessel expansion phase, with timing shifting along the ring, according to the moment of vessel expansion. Regional differences were significant, but low, compared with the effect of chronology type. A large part of the variance explained by region was due to the strong difference between Western Pyrenees forests –growing under hyperhumid conditions– and the rest of forests under drier and warmer climate. Only minor differences between altitudes were found for the climate control of ring width and vessel size at annual scale, and no intra-annual effect on climate control of MVA. The stronger effect of chronology type on climatic response compared to the role of geographical location or altitude suggests common climate constraints on secondary growth and xylem anatomy along beech dry edge.

1. Introduction

The western Mediterranean Region is suffering the effects of climate warming due to a faster than average increase in mean temperature (Cramer et al., 2018). A warmer climate raises evapotranspiration rates, which frequently combined with reduced rainfall, amplify vegetation sensitivity to drought (Dai et al., 2018). The frequency and intensity of extreme drought events is also rising in southern Europe (Spinoni et al., 2018), leading to effects at multiple temporal scales, from sharp growth reductions to progressive decreases in tree vitality, potentially reaching tipping points (Rever et al., 2015), and driving tree dieback and mortality in some cases (Allen et al., 2010; Hartmann et al., 2018; Hammond et al., 2022). The response of tree species to climate warming will depend on their structural and functional plasticity (Greenwood et al., 2017), and those species most sensitive to drought are expected to diminish their share on forest composition (Etzold et al., 2019). In this sense, temperate tree species inhabiting areas within or close to the Mediterranean Region are prone to be displaced by climate warming due to their lower tolerance to drought than Mediterranean species (Jump et al., 2006; Camarero et al., 2010).

Iberian European beech (*Fagus sylvatica* L.) populations are strong candidates to be severely affected by a warmer and drier climate (Jump et al., 2006; Piovesan et al., 2008). A warmer and drier climate is expected to produce growth declines (Martínez del Castillo et al., 2022),

Abbreviations: MVA, Mean Vessel Area; RW, Ring Width.

* Corresponding author.
E-mail address: josemiguel.olano@uva.es (J. Olano).

https://doi.org/10.1016/j.agrformet.2022.109082
Received 11 March 2022; Received in revised form 20 May 2022; Accepted 5 July 2022
Available online 16 July 2022

reduced recruitment rates (Bolte et al., 2016) and higher mortality (Leuschner 2020). Beech reaches its southwestern range edge in the Iberian Peninsula, where summer conditions are drier than in its core area. In fact, a large part of Iberian beech populations already grows under unfavorable macroclimate conditions, being restricted to mountain areas with higher pluviometry and/or frequent fogs to temper summer drought intensity (Costa et al., 1997; Rozas et al., 2015). It is predicted that the climatic context for these species will worsen in future decades (IPCC 2021). Thus, the persistence of southern beech populations is being challenged by a combination of higher drought stress in their lower-elevation populations (Serra-Maluquer et al., 2019) and more frequent late-spring frost defoliations in the upper beech altitudinal limit (Olano et al., 2021; Sangüesa-Barreda et al., 2021). Some authors indicated that a withdrawal in the beech lowest/driest localities is already occurring (Jump et al., 2006; Piovesan et al., 2008, but see Hacket-Pain and Friend, 2017; Sánchez et al., 2021). However, the final outcome of the interaction between beech and a novel climate scenario will depend on their ability to adjust its life stages to increasing drought levels. In this sense, beech response to drought shows a high phenotypic plasticity (Aranda et al., 2017; Herbette et al., 2021) as well as a marked intraspecific genetic differentiation (Pluess and Weber 2012, Pfenninger et al., 2021, Postolache et al., 2021) to deal with drought. Plastic responses of beech to climate fluctuations can also be appreciated in the inter-annual variation of xylem anatomy and xylogenesis (Sass and Eckstein 1995; Prislan et al., 2013, Zimmermann et al.,2021).

Time series of annual secondary growth are routinely used to understand the climatic constraints of tree growth along environmental gradients as well as its temporal shifts (Di Filippo et al.,2007), providing a useful tool to reconstruct tree response to climate, but also to forecast tree responses to expected climatic trends (Sánchez-Salguero et al., 2016). The developing field of quantitative wood anatomy provides a complementary framework to understand tree physiological responses to climate variation (Fonti et al., 2010), since plant may adjust their xylem anatomy in response to climate fluctuations (e.g., producing wider vessels when water availability is higher). Changes in xylem anatomy have direct implications in hydraulic function (Sperry et al., 2008) and enable to track how species adjust their hydraulic structure to different climatic conditions both spatially (García-Cervigón et al., 2018, 2020) and temporally (Arnič et al., 2021; Olano et al., 2012).

Our aim was to explore the climate control on ring width (RW) and mean vessel area (MVA) along beech altitudinal and latitudinal distribution range in the Iberian Peninsula. The mechanism behind vessel expansion is relatively well understood with cell turgor playing a primary role, thus it can be clearly linked to environmental variability (Rathgeber et al., 2016). Moreover, previous studies indicate that MVA variability in beech is independent of secondary growth rate variation (Arnič et al., 2021; Sass and Eckstein, 1995), thus both traits might provide complementary information. We selected four mountain areas to include the existing geographic variability in southwestern beech populations, three of them located in the species' Mediterranean limit, where summer droughts are frequent, and a fourth region under climatic conditions close to the species optimum in the Western Pyrenees under hyperhumid Eurosiberian climate. Within each area we selected two populations at contrasting elevation to explore the altitudinal variability of climate constraints and their potential effects on wood traits.

Based on the existing knowledge about our study species, we hypothesized that inter-annual variability of MVA is affected by hydraulic pressure control on vessel expansion (Rathgeber et al., 2016; Peters et al., 2020), and therefore it will be strongly dependent on factors controlling soil moisture during the growing season. In contrast, we hypothesized that RW depends climate factors promoting resource levels (carbohydrates) acquisition to support ring formation (von Arx et al., 2017), as well as on climatic conditions that mitigate water stress and promote cambial activity length and intensity during the growing season (Rozas et al., 2015; Hacket-Pain et al., 2016). If secondary growth is controlled by cambial activity constraints, MVA and RW control will occur over the same temporal domain and they may share a large part of their climatic signals. However, if factors related to resource availability have a stronger role in driving RW, we expect that a large part of the climate signals of RW and MVA will differ. Additionally, we hypothesized that factors controlling MVA may reflect the hydraulic conditions during the xylogenetic phase of conduit expansion (Arnič et al., 2021; Olano et al., 2012). We expect that the timing of climatic control will shift from the onset of xylogenesis at the beginning of the ring to the cessation of ring expansion at the end of the ring, with a time domain that will shift from May to July (August), according to cambial phenology of beech in the study area (Martínez del Castillo et al., 2016). We also hypothesized these signals will be modulated by region and altitude, with stronger water limitation in populations at low altitude and close to the Mediterranean dry limit of beech distribution.

2. Material and methods

2.1. Study area and sampling design

We sampled beech forests in four mountain ranges across the southwestern *Fagus sylvatica* distribution area (Fig. 1). Three of the mountains represented the southern Iberian limit of the species (Cantabrian Range, Iberian Range and Moncayo mountain) in close contact with the Mediterranean bioclimatic Region, whereas the last one (Western Pyrenees) was under hyperhumid Eurosiberian climate with high annual and summer precipitation levels. Mean annual temperature ranges from 5.1 ℃ at high Western Pyrenees site to 9.4 ℃ at low Iberian Range site. Precipitation shows a large gradient (Table 1, Fig. 1), from 2187 mm per year (557 from June to August) in the highest Western Pyrenees site to less than a third (657 mm per year, 236 from June to August) in the lowest Moncayo site.

In each mountain range we selected four plots of mature forests at different altitudes. Two plots were close to the upper limit of the continuous forest distribution and two were at lower altitudes (Fig. 1). The altitude difference between both altitudes was at least 300 m a.s.l. In each plot we selected eight dominant or codominant trees, and each tree was georeferenced with submeter level accuracy using a GPS (Trimble Geo 7X). We extracted three wood cores at 1.3 m height from each tree using Pressler increment borers. Sampling took place in 2017 and 2018, although some trees were revisited in 2019 to extract additional cores in cases the previously extracted cores lacked enough quality.

2.2. Ring width chronologies

Two increment cores per tree were air-dried and mounted on wooden supports and progressively sanded until cellular structure could be assessed in transverse section. Samples were visually cross-dated and measured at a minimum resolution of 0.01 mm using a VELMEX (Inc., USA) measuring system. Cross-dating quality was checked with the COFECHA program (Holmes, 1983). We standardized ring width time series to obtain dimensionless ring-width chronologies without temporal autocorrelation. We removed long term trends and tree age/size effects on annual ring width using a linear or negative exponential function. After this procedure, we applied a cubic smoothing spline with a 50% frequency response cut-off of 32 years. Finally, we removed first-order autocorrelation in the resulting series, obtaining a residual chronology. We calculated the Explained Population Signal (EPS) for each residual chronology to estimate chronology common signal (Table 1). These analyses were performed using the dplR package (Bunn, 2008) in R environment (R Core Team, 2020).

2.3. . Mean vessel area chronologies

Anatomical wood cross-sections of 10 μm thickness from cores were produced with a sledge microtome (Gärtner et al., 2015). Since cores were too large to be cut with the microtome, we miter cut them into

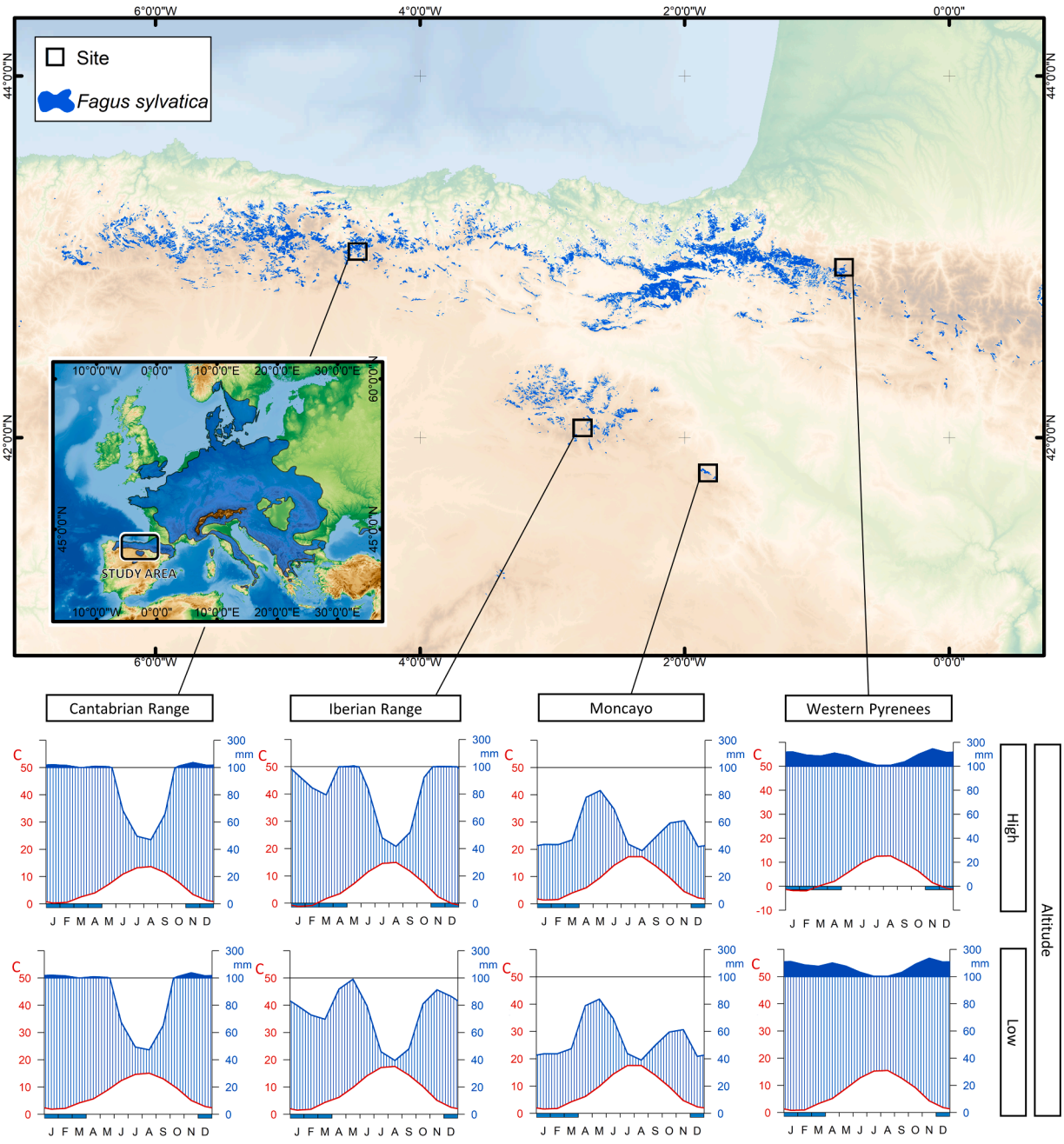

Fig. 1. Location and climodiagrams of the sampling sites along the study area. Beech distribution map according to Caudullo et al. (2017).

Table 1
Altitude and meteorological traits of the sampling sites and statistics of the RW and MVA chronologies. RW: Ring width, MVA: mean vessel area considering the whole growth ring, EPS: expressed population signal. Annual and summer (June - August) precipitation and mean temperature obtained from gridded data from CHELSA v2.1 for the 1980–2018 period (Karger et al., 2017, 2018). This climatic repository provides higher spatial resolution (1 km) but does not fully cover the study period (1950–2017).

Region		Altitude (m)	Annual/Summer P (mm)	Mean T (°C)	Period	#trees/series		EPS	
						RW	MVA	RW	MVA
Cantabrian Range	High	1369	1166/274	7.0	1751–2018	15/29	10	0.89	0.38
	Low	1045	1163/271	8.5	1790–2018	16/30	10	0.86	0.52
Iberian Range	High	1599	994/282	6.7	1785–2017	16/38	8	0.90	0.27
	Low	1261	885/264	9.4	1636–2017	15/32	9	0.85	0.42
Moncayo	High	1565	657/236	9.0	1805–2017	17/41	10	0.95	0.58
	Low	1364	660/236	9.3	1810–2017	16/37	9	0.93	0.52
Western Pyrenees	High	1601	2187/557	5.1	1713–2017	15/29	10	0.88	0.59
	Low	1399	2157/524	8.1	1583–2017	16/31	10	0.90	0.47

smaller pieces to avoid annual rings loss. These cross-sections were then placed on a slide and stained with Alcian blue (1% solution in acetic acid) and safranin (1% solution in ethanol). The cross-sections were submerged in ethanol solutions of increasing concentration, washed with xylol and permanently preserved by embedding them in Eukitt glue. Overlapping images covering a complete radius from pith to bark were captured with a Nikon D90 digital camera mounted on a Nikon Eclipse 50i optical microscope with 40× magnification resulting in 1.63 μm per pixel resolution. Photographs were merged to a single image using PTGUI v8.3.10 Pro (New House Internet Services B.V., Rotterdam, The Netherlands).

We identified vessel outlines using ROXAS v3.0 (von Arx and Dietz, 2005), a specific image-analysis tool based on Image-Pro Plus (Media Cybernetics, Silver Spring, MD, USA). We first adjusted ROXAS settings to create different configurations of parameters for automatic vessel extraction. We performed a preliminary visual exploration to adjust the maximum and minimum vessel size, vessel ovality and several color parameters. We used these configurations to automatically analyze all samples. The automatic output was then manually edited by drawing ring boundaries, deleting erroneously detected vessels (e.g. in parenchyma rays), and rectifying further misidentifications. For each vessel, we obtained its area as well as the distance of its centroid from the corresponding ring boundary. We averaged vessel area per ring to create a mean vessel area (MVA) chronology. Additionally, we calculated an additional ring-width (RW) chronology for each individual from anatomical cross-sections and related them to previously developed ring-width chronologies. Finally, we built a residual chronology following the same procedure as for ring width data. Residual chronologies enabled to remove tree height effects on vessel size (Olson et al., 2021) as well as extracting high frequency signal linked to inter-annual variability.

In order to establish the intra-annual factors affecting mean vessel size, we divided each ring in three segments. First, we set a limit at 70% of ring width, separating the last 30% as the final part of the ring where vessel size diminishes. Then, we divided the earlier 70% part of the ring in two halves of 35%. Each vessel was attributed to one of the three sections (S1 at 0–35%, S2 at 35–70%, S3 at 70–100%) considering the position of its center in relation to ring boundaries. Finally, we calculated one MVA residual chronology for each of the three sections. Since chronologies of contiguous sections are highly correlated (up to 0.66) due to a carry-over effect on mean vessel area, we removed its mutual dependence by extracting the residuals of the regression between each section and the previous one (S2 vs. S1, S3 vs. S2) and dividing it by the predicted value (Arzac et al., 2018). This procedure provided uncorrelated residual chronologies of MVA for each section.

2.4. . Climate growth correlations

We downloaded monthly gridded data from the datasets of the Climate Research Unit, University of East Anglia (https://crudata.uea.ac.uk/; CRU TS 4.05, 0.5° × 0.5°; Harris et al., 2020), for mean temperatures and total precipitation in the period 1950–2017, as it fulfills all requirements for the subsequent analyses regarding timespan and availability. Relations between climate, tree growth and MVA were explored from June of the year previous to growth (JUN) to August of the growth year (Aug) using monthly values and obtaining Pearson's correlations. We set this period to check for previous summer and autumn effects on tree growth and anatomy until August, when xylogenesis ends in our study area (Martínez del Castillo et al.,2016).

2.5. . Multivariate analysis of climate response

We used multivariate analyses to disentangle the effect of chronology type (RW, MVA) on climate response matrix. We performed a principal component analysis (PCA) on the chronology × climate correlation matrix. Climate response matrix included correlation coefficient derived values to monthly total precipitation and mean monthly temperature from previous June to August of the growing season. Since Pearson's r coefficient shows a quadratic relation to the explained variations, we used r^2 values instead of r. To distinguish between positive and negative effects, we divided r^2 by the sign (positive or negative) of the correlation. We performed this procedure: (1) to assess the difference in the climatic control on RW and MVA in the whole ring, and (2) to assess the difference in the climatic control on MVA along the three different and consecutive sections of the ring.

To disentangle the effects of each chronology type, region and relative altitude on climate response matrices, we performed a redundancy analysis (RDA). This technique combines multiple regression with PCA, relating the dependent matrix (chronology × climate) to an explanatory matrix that was comprised of three components: region (a dummy variable with three levels), altitude (a binary variable) and chronology type (RW and MVA). Chronology was considered a binary variable (RW/MVA) in whole ring analysis but as a discrete parameter (1, 2, 3) for the three consecutive sections of MVA chronologies. The significance of the whole model, as well as of each explanatory variable, was evaluated by means of Monte Carlo tests with 9999 permutations. Then, we performed partial redundancy analyses (pRDA) to assess the contribution of each explanatory variable to the dependent matrix. For each pRDA, the dependent matrix was constrained by each of the explanatory variables and controlled for the remaining variables. Adjusted R^2 values were obtained with the function *RsquareAdj()*, and multivariate analyses were performed with the *vegan* R package (Oksanen et al., 2020).

3. Results

3.1. . Ring width and mean vessel area chronologies

We measured a total of 45,897 rings from 126 trees (267 cores) and 5.5 million vessels from 76 trees, leading to 8 RW (Fig. S1) and 8 MVA chronologies (Fig. S2). The largest chronology lasted from 1583 to 2020 (Western Pyrenees low; Table 1), although we focused on the 1950–2017 period. Mean tree ring width was 1.11 ± 0.78 mm and mean vessel area, 1220.70 ± 514.60 μm^2, with decreasing size along ring sections (S1: 1321.48 ± 664.82 μm^2, S2: 1194.45 ± 591.91 μm^2, S3: 764.08 ± 382.72 μm^2; see data per site at Table S1). All RW chronologies achieved EPS values larger than 0.85 (Wigley et al., 1984). MVA chronologies showed much smaller EPS values (0.274–0.587), in agreement with existing literature on vessel traits (Oladi et al., 2014). Similar low EPS values were found for the 3 MVA chronologies per tree ring fraction.

3.2. . Ring width and mean vessel area climatic response

Ring width responded positively to precipitation during previous summer in the three southern mountain ranges (Fig. 2). The effect extended to July in 5 out of 8 sites and to August in 3 sites. A detrimental effect of mean temperature during the previous summer on ring width was found, but with a low impact just in two Mediterranean sites, being stronger in August (Fig. S3). Surprisingly, precipitation during the growing season had a small impact on tree ring width, being relevant in April, prior to leaf flushing, in 5 out of 8 sites, and only in one site during the growing period, in June at low altitude in the Cantabrian Range. High temperatures in May promoted growth in just 3 sites (Fig. S3).

Regarding MVA, previous year precipitation exerted little effect in the high Pyrenean site, being positive in June and negative in July (Figs. 2, S3). In contrast, conditions during the growing season had a strong effect on MVA. Overall, wet conditions in current May and July favored the formation of larger vessels in all sites except the high Pyrenean site, where the positive effect was restricted to April. Mean temperature had a less clear pattern with positive effects in February in two sites (Moncayo and Cantabrian Range). In the lowest Mediterranean edge sites (Iberian and Cantabrian Range), July-August temperatures

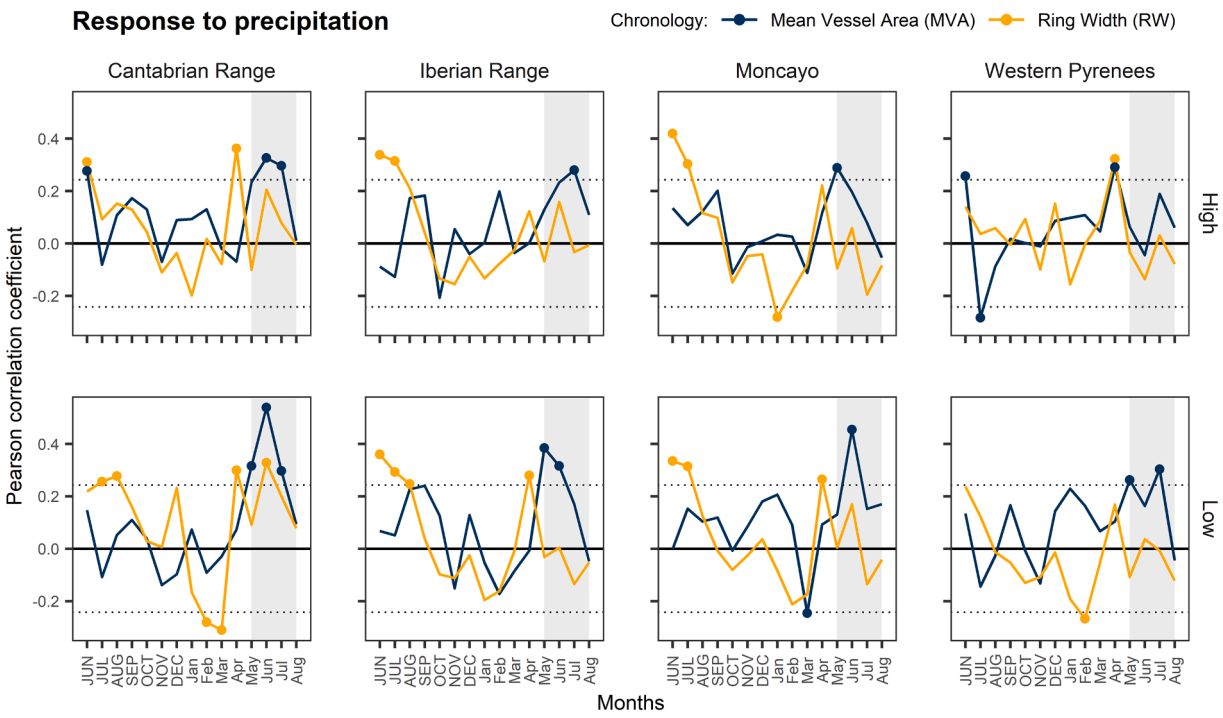

Fig. 2. Pearson correlations between residual chronologies of ring width and whole ring MVA (see legend above) with monthly precipitation from previous year (uppercase) June to growing year (lower case) August for each site and altitude. Dotted line indicates the threshold for $P < 0.05$. Shaded area indicates the xylogenesis period for beech in the study area, according to Martínez del Castillo et al. (2016).

had strong negative effects on MVA.

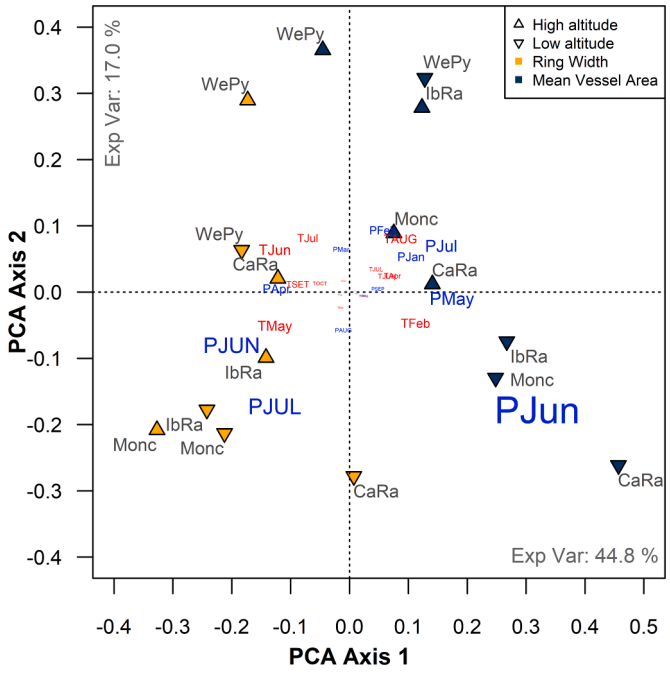

Fig. 3. PCA biplot of chronology-climate response matrix for ring width (pale brown) and MVA (dark blue) residual chronologies (legend above). Up oriented triangles indicate high altitude and down oriented triangles low altitude plots. Regions are indicated with short names CaRa (Cantabrian Range), IbRa (Iberian Range), Monc (Moncayo) and WePy (Western Pyrenees). Blue (precipitation) and red (mean temperature) text indicate the position of climate parameters, and characters' size is proportional to their contribution to the ordination. Numbers in the inner part of the axes indicate the percentage of explained variance.

The disparate response of MVA and RW to climate was evidenced by the PCA biplot (Fig. 3). First axis discriminated between RW and MVA chronologies and comprised 44.8% of the total variance (Fig. 3). Second PCA axis accounted for a much lower explained variance (16.9%) mainly responding to the geographic location of the sites, with W Pyrenees reaching the highest values. The most relevant climatic factors determining PCA structure were related to precipitation. RW chronologies were highly correlated with June and July precipitation in the previous year and, to a lower extent, with April precipitation and May and June temperature in the growth year. MVA chronologies responded mostly to precipitation (May-July), and to August temperature in the previous year. pRDA results showed that the chronology type, region and altitude explained as much as 65.5% of the 8 × 30 chronology-climate response matrix. Chronology type had by far the largest explanatory power (33.7%; Table 2), a proportion that increased to 41% when the effects of region and altitude were controlled. Region

Table 2
RDA variance explained by environmental parameters on chronology-climate response matrix for RW residual and whole ring MVA chronologies. Full model indicates the variance explained by the contribution of all the constraining factors. *Single* column shows the variance explained by each factor alone, whereas *Conditional* column indicates the variance explained by each factor after removing the effect of the other two parameters. χ^2, F and *P* correspond to the significance of the factor effect after considering the effect of the rest of the factors and evaluated through 9999 Monte Carlo permutations. RW/MVA is a binary parameter explaining the identity of the chronology, region is a nominal parameter relating to region identity and altitude is a binary parameter indicating whether the sampling site is in the low or high position within the region.

RW/MVA pRDA	*Explained variance*		*df*	χ^2	*F*	*P*
	Single	*Conditional*				
RW/MVA	0.337	0.410	1	$33.8 * 10^{-5}$	9.78	<0.001
Region	0.236	0.156	3	$23.9 * 10^{-5}$	2.30	<0.001
Altitude	0.082	0.065	1	$8.3 * 10^{-5}$	2.39	0.017
Full Model	0.655					

explained just 15.6% of the variance after controlling for other factors? effects. Finally, altitude explained 6.5% of the variance, albeit its effect was significant.

3.3. . Sequential mean vessel area chronologies climatic response

The decomposition of MVA into three different sections/chronologies (S1, S2 and S3) showed a positive effect of May precipitation on S1 in 6 out of 8 sites (Figs. 4, S4). This effect extended into June in two of the lowest sites (Cantabrian Range and Moncayo). The precipitation signal moved to June in S2 in the Mediterranean edge mountains (4 out of 6 plus one marginal), but not in the Pyrenees highest population. Finally, S3 had no summer precipitation signals in Pyrenees but showed positive effects of June (4 out of 6), July (5 out of 6) and even August (1 out of 6) in the Mediterranean edge mountains. Previous July precipitation contributed negatively in MVA just in the Pyrenean sites, while a positive effect of previous June precipitation was detected only in the Cantabrian Range. Mean temperature showed a lower impact in MVA, with a positive effect of April temperature in S3 in the three Mediterranean sites and a negative effect of summer temperature in Cantabrian and Iberian Ranges.

This sequential pattern agreed with that observed for the climate response correlation matrix between MVA residual chronologies along different sections within the ring (Fig. 5). First axis comprised 34.5% of the total variance, discriminating S1 chronologies with strong May precipitation positive signals from the rest. S2 and S3 chronologies did not show such a clear pattern, albeit S3 chronologies tended to show higher values in the first PCA axis. These chronologies were correlated with June precipitations during the growth year. The second axis explained just 16% of the variance and did discriminate Pyrenean sites in the upper values.

The pRDA analysis showed a preponderance of ring position in the structure of MVA climate response signal (Table 3). This factor explained 21.4% of the variance and was three times as important as the following one (region) which accounted for just 7.7% of the variance

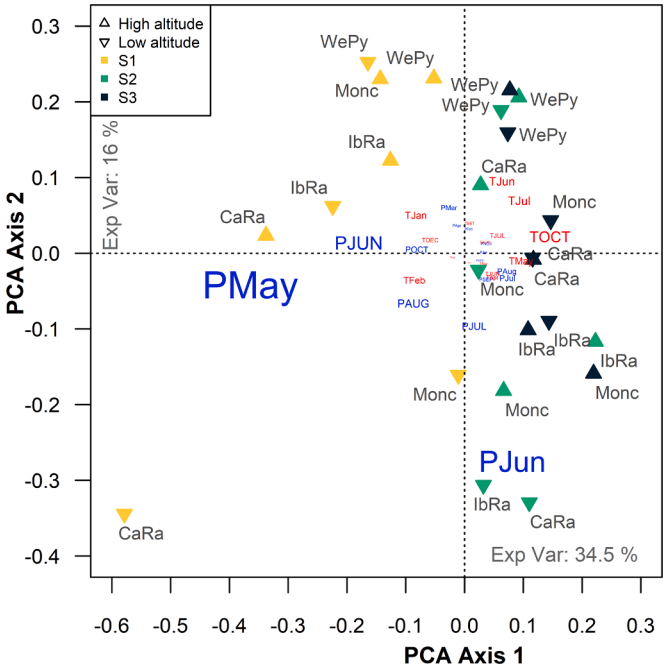

Fig. 5. PCA biplot of the climate response correlation matrix for MVA residual chronologies along different sections within the ring. Colors correspond with ring sections (see legend above): first section (S1: 0–35%; yellow), second (S2: 35–70%; green) and last section (S3: 70–100%; black). Up-oriented triangles indicate high altitude and down-oriented triangles, low altitude plots. Blue (precipitation) and red (mean temperature) text indicate the position of climate parameters, and characters' size is proportional to climate parameter contribution to the ordination. Numbers in the inner positive part of the axes indicate the explained variance of each axis.

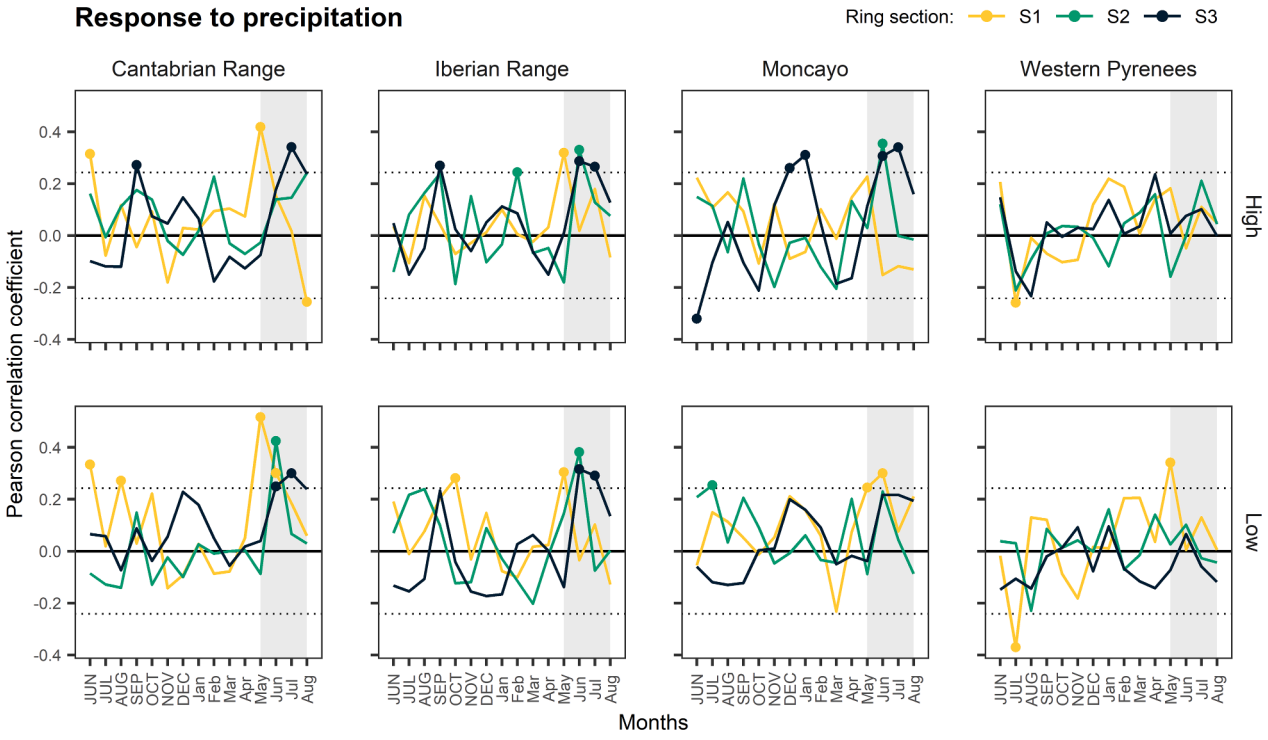

Fig. 4. Pearson correlations between residual chronologies of MVA along different sections of the annual ring (Sections 1 (yellow), 2 (green) and 3 (black); color legend above) with monthly precipitation from previous year June to growing year August. Horizontal dotted lines indicate the threshold for $P < 0.05$. Shaded area indicates the xylogenesis period for beech in the study area, according to Martínez del Castillo et al. (2016).

Table 3
RDA variance explained by environmental parameters on climate response correlation matrix for MVA residual chronologies along different sections within the annual ring. Full model indicates the variance explained by all the environmental parameters. Single column shows the variance explained by each parameter alone, whereas conditional column indicates the variance explained by each parameter after removing the effect of the other two parameters. χ^2, F and *P* correspond to the significance of parameters effect after considering the effect of the rest evaluated through 9999 Monte Carlo permutations. Position is an ordinal parameter responding to the position along the tree ring (1,2,3), region is a nominal parameter relating to region identity and altitude is a binary parameter indicating whether the sampling site is in the low or high position within the region.

Sequential MVA pRDA	*Explained variance*		*df*	χ^2	*F*	*P*
	Single	*Conditional*				
Ring position	0.210	0.214	1	17.2 $*10^{-5}$	9.78	<0.001
Region	0.168	0.077	3	13.9 $*10^{-5}$	2.30	0.009
Altitude	0.031	0	1	2.6 $*10^{-5}$	2.39	0.493
Full Model	0.412					

once the effect of chronology type and altitude were controlled. Interestingly, altitude had no significant effect. It is important to note that ring position was included as an ordinal parameter, whereas region was a dummy factor with three levels.

4. Discussion

Secondary growth and mean vessel area (MVA) were controlled by precipitation at different time domains in beech's southwestern distribution range. Secondary growth responded primarily to precipitation in the previous growing season, whereas MVA increased with water availability during vessel expansion. The MVA climate signal shifted along the tree ring, recording the hydraulic conditions in which cell expansion of each section occurred. The role of region and altitude determining climate response was minor compared to chronology type, but strong differences occurred between populations close to Mediterranean conditions and in the hyperhumid Western Pyrenees.

Precipitation during late spring and early summer was correlated with inter- and intra-annual variability in MVA. Wetter conditions increase soil moisture reducing root-to-leave water potential gradient, promoting cell turgor, a critical factor to promote vessel expansion of developing xylem conduits (Steppe et al., 2015). Wetter conditions increase soil moisture reducing root-to-leave water potential gradient, promoting cell turgor and conduit expansion. When MVA value for the whole ring was considered, the main signal corresponded to May-June precipitation, which represents the period when the largest part of the ring is formed (Martínez del Castillo et al., 2016). After splitting the ring in three different sections, removing intra-annual autocorrelation and isolating the climate signal along the temporal sequence of ring formation, the precipitation effect moved from May to July, and eventually to August, mirroring the period in which xylogenesis and vessel expansion occur along the ring (Martínez del Castillo et al., 2016). Our results match the pioneering study of Sass and Eckstein (1995) that also found a positive effect of precipitation on beech xylem vessel size at its core distribution area, and shows a pattern that has also been reported for tracheids in a Mediterranean gymnosperm (Olano et al., 2012). However, it contrasts with previous works in beech that postulate that MVA climate signal is concentrated just in the last segments of the ring, while initial parts are under internal control (Pourtahmasi et al., 2011; Prislan et al., 2018). The presence of a strong precipitation signal in MVA may reflect the variability of climate constraints to vessel expansion along beech distribution. Dry edge populations experience higher water limitation than core populations. In this sense, the identification of a precipitation signal in MVA for a submediterranean beech population (Arnič et al., 2021), as well as the absence of precipitation signal in the highest site in the Western Pyrenees, would support a stronger climate control on vessel expansion for rear edge populations.

Beech secondary growth showed a lagged response to late spring-early summer precipitation in the year previous to growth, corroborating the relevance of previous year conditions on beech secondary growth (Hacket-Pain et al., 2016). However, our results did not show a climate signal related to temperature (Hacket-Pain et al., 2016). Previous year signal was related to precipitation, in agreement with previous works at the rear edge of beech distribution (Piovesan et al., 2008; Chen et al., 2015; Rozas et al., 2015; Martínez del Castillo et al., 2018, 2019). A potential explanation might relate the existence of larger vessel diameters to higher water availability during the previous growing season, which results in improved xylem conductivity. Indeed, larger conductivity due to higher vessel size has been linked to growth potential in temperate ring-porous species (Klesse et al., 2021; Pérez-De-Lis et al., 2016). Nevertheless, this relationship may not hold for diffuse-porous species, since sapwood rings remain functional reducing the effect of a single year on whole stem conductivity (Gasson, 1985).

Non-structural carbohydrates (NSC) availability seems an alternative mechanism to explain the effect of previous year conditions on next year growth (von Arx et al.,2017), with two plausible and non-exclusive hypotheses. Warm and dry summers trigger next year investment in beech reproduction (Kabeya et al., 2017), leading to masting episodes (Chiavetta and Marzini 2021) and reducing NSC available for secondary growth (Hacket-Pain et al., 2018). However, we found no effect of previous year temperature (the main climatic trigger of masting events) on secondary growth. Alternatively, wet conditions during summer increase photosynthetic rates as well as a longer vegetative period (Estiarte and Peñuelas, 2015; Gárate-Escamilla et al., 2020), result in higher NSC pools. Xylogenesis pace is very dependent on carbohydrates (Oberhuber et al., 2011) and elevated NSC levels might be critical to promote a higher xylem cell formation rate (Deslauriers et al., 2009). Beech secondary growth occurs over a short period in the species southern range (Larysch et al., 2021; Martínez del Castillo et al., 2016; Prislan et al., 2018, 2019), in such a way that inter-annual differences in secondary growth would be more dependent on growth rate variability than on the growing season length (Prislan et al., 2013; Kabeya et al., 2017), thus resulting in higher annual rings in years with higher NSC levels.

Altitude and geographical location explained very small fractions of the climate response. The low variability of altitude is surprising, since there is ample evidence showing that limiting factors for tree growth shift along altitudinal gradients in Mediterranean mountains, with the upper species limit being constrained by temperature, and upper areas by water availability (Arzac et al., 2016), as has also been reported for beech (Martínez del Castillo et al., 2019) Moreover, the onset of cambial activity is strongly dependent on temperature (Rossi et al., 2008), leading to earlier cambial onsets and longer growing seasons at lower altitudes (Martínez del Castillo et al., 2016; Moser et al., 2010). Nevertheless, only minor differences between altitudes were found for the climate control of secondary growth and vessel size at annual scale, and no intra-annual effect on vessel size climate control was found. However, we did not consider other climate factors like extreme temperatures and late frosts occurrence, which do have a differential effect along altitudinal gradients (Arzac et al., 2016; Olano et al., 2021). Regional differences were significant, but low, compared with the effect of chronology type, with a large part of this variance being attributed to the strong difference between Western Pyrenees forests growing under hyperhumid conditions and the rest of forests growing under a drier macroclimate and sharing a common signal.

5. Conclusions

Our findings demonstrate that secondary growth and mean vessel area encode disparate climate signals along *Fagus sylvatica* southwestern

distribution edge. Vessel area was correlated to short term variation of hydraulic conditions during the vessel expansion phase in response to water availability. In contrast, the lagged effect of water availability during previous growing season was the most relevant factor explaining ring-width variability. The combination of vessel anatomy and ring width improved our ability to decode the environmental drivers of European beech secondary growth in the species dry distribution edge.

Funding

Spanish Ministerio de Ciencia e Innovación [CGL2017-87309-P; PID2020-118444GA-100; PID2019-109906RA-I00; PRE2018-084106 to MG-H]; Spanish Ministerio de Economía, Industria y Competitividad [IJC2019-040571-I to GS-B]; Junta de Castilla y León-Consejería de Educación [IR20201-UVA08; VA171P20) and EU LIFE Soria Forest Adapt [LIFE19 CCA/ES/001181] and UE FEDER Funds.

Declaration of Competing Interest

The authors declare that they have no known competing financial interests or personal relationships that could have appeared to influence the work reported in this paper.

Acknowledgments

We thank Environmental Services of Castilla y León (Palencia, Soria services), La Rioja, Aragón and Navarra for sampling permissions and to environmental agents for field assistance and indications. We thank Alfonso Martínez and Juan Carlos Rubio for assistance with core processing.

Data and materials availability

Data will be available upon request and stored in Figshare (https://figshare.com/) after article acceptance

Supplementary materials

Supplementary material associated with this article can be found, in the online version, at doi:10.1016/j.agrformet.2022.109082.

References

Allen, C.D., Macalady, A.K., Chenchouni, H., Bachelet, D., McDowell, N., Vennetier, M., Kitzberger, T., Rigling, A., Breshears, D.D., Hogg, E.H., Gonzalez, P., Fensham, R., Zhang, Z., Castro, J., Demidova, N., Limp, J.H., Allard, G., Running, S.W., Semercis, A., Cobb, N., 2010. A global overview of drought and heat-induced tree mortality reveals emerging climate change risks for forests. For. Ecol. Manag. 259, 660–684.

Aranda, I., Bahamonde, H.A., Sánchez-Gómez, D., 2017. Intra-population variability in the drought response of a beech (*Fagus sylvatica* L.) population in the southwest of Europe. Tree Physiol. 37, 938–949.

Arnič, D., Gričar, J., Jevšenak, J., Božič, G., von Arx, G., Prislan, P., 2021. Different wood anatomical and growth responses in european beech (*Fagus sylvatica* L.) at three forest sites in Slovenia. Front. Plant Sci. 12, 1551.

Arzac, A., Garcia-Cervigon, A.I., Vicente-Serrano, S.M., Loidi, J., Olano, J.M, 2016. Phenological shifts in climatic response of secondary growth allow *Juniperus sabina* L. to cope with altitudinal and temporal climate variability. Agric. For. Meteorol. 217, 35–45.

Arzac, A., Rozas, V., Rozenberg, P., Olano, J.M., 2018. Water availability controls *Pinus pinaster* xylem growth and density: a multi-proxy approach along its environmental range. Agric. For. Meteorol. 250, 171–180.

Bolte, A., Czajkowski, T., Cocozza, C., Tognetti, R., de Miguel, M., Pšidová, E., Ditmarová, Ľ., Dinca, L., Delzon, S., Cochard, H., Ræbild, A., de Luis, M., Cvjetkovic, B., Heiri, C., Müller, J., 2016. Desiccation and mortality dynamics in seedlings of different european beech (*Fagus sylvatica* L.) populations under extreme drought conditions. Front. Plant Sci. 7.

Bunn, A.G., 2008. A dendrochronology program library in R (dplR). Dendrochronologia 26, 115–124.

Camarero, J.J., Olano, J.M., Parras, A., 2010. Plastic bimodal xylogenesis in conifers from continental Mediterranean climates. New Phytol. 185, 471–480.

Caudullo, G., Welk, E., San-Miguel-Ayanz, J., 2017. Chorological maps for the main European woody species. Data Brief 12, 662–666.

Chen, K., Dorado-Liñán, I., Akhmetzyanov, L., Gea-Izquierdo, G., Zlatanov, T., Menzel, A., 2015. Influence of climate drivers and the North Atlantic Oscillation on beech growth at marginal sites across the Mediterranean. Clim. Res. 66, 229–242.

Chiavetta, U., Marzini, S., 2021. foreMast: an R package for predicting beech (*Fagus sylvatica* L.) masting events in European countries. Ann. For. Sci. 78, 93.

Costa, M., Morla, M., Sainz, H., 1997. Los Bosques Ibéricos. Planeta. Ed.

Cramer, W., Joel, G., Fader, M., Garrabou, J., Gattuso, J.-P., Iglesias, A., Lange, M., Lionello, P., Llasat, M., Paz, S., Peñuelas, J., Snoussi, M., Toreti, A., Tsimplis, M., Xoplaki, E., 2018. Climate change and interconnected risks to sustainable development in the Mediterranean. Nat. Clim. Chang. 8, 972–980.

Dai, A., Zhao, T., Chen, J., 2018. Climate change and drought: a precipitation and evaporation perspective. Curr. Clim. Chang. Rep. 4, 301–312.

Deslauriers, A, Giovannelli, A, Rossi, S, Castro, G, Fragnelli, G, Traversi, L, 2009. Intra-annual cambial activity and carbon availability in stem of poplar. Tree Physiol. 29, 1223–1235. https://doi.org/10.1093/treephys/tpp061.

Di Filippo, A., Biondi, F., Cufar, K., De Luis, M., Grabner, M., Maugeri, M., Saba, E., Schirone, B., Piovesan, G., 2007. Bioclimatology of beech (*Fagus sylvatica* L.) in the Eastern Alps: spatial and altitudinal climatic signals identified through a tree-ring network. J. Biogeogr. 34, 1873–1892.

Estiarte, M., Peñuelas, J., 2015. Alteration of the phenology of leaf senescence and fall in winter deciduous species by climate change: effects on nutrient proficiency. Glob. Chang. Biol. 21, 1005–1017.

Etzold, S., Ziemińska, K., Rohner, B., Bottero, A., Bose, A., Ruehr, N., Zingg, A., Rigling, A., 2019. One century of forest monitoring data in Switzerland reveals species- and site-specific trends of climate-induced tree mortality. Front. Plant Sci. 10, 307.

Fonti, P., von Arx, G., García-González, I., Eilmann, B., Sass-Klaassen, U., Gärtner, H., Eckstein, D., 2010. Studying global change through investigation of the plastic responses of xylem anatomy in tree rings. New Phytol. 185, 42–53.

Gárate-Escamilla, H., Brelsford, C., Hampe, A., Robson, T., Benito-Garzon, M., 2020. Greater capacity to exploit warming temperatures in northern populations of European beech is partly driven by delayed leaf senescence. Agric. For. Meteorol. 284, 107908.

García-Cervigón, A.I., Fajardo, A., Caetano-Sánchez, C., Camarero, J.J., Olano, J.M., 2020. Xylem anatomy needs to change, so that conductivity can stay the same: xylem adjustments across elevation and latitude in *Nothofagus pumilio*. Ann. Bot. 125, 1101–1112.

García-Cervigón, A.I., Olano, J.M., von Arx, G., Fajardo, A., 2018. Xylem adjusts to maintain efficiency across a steep precipitation gradient in two coexisting generalist species. Ann. Bot. 122, 461–472.

Gärtner, H., Lucchinetti, S., Schweingruber, F.H., 2015. A new sledge microtome to combine wood anatomy and tree-ring ecology. IAWA J. 36, 452–459.

Gasson, P., 1985. Automatic measurement of vessel lumen area and diameter with particular reference to pedunculate oak and common beech. IAWA J. 6, 219–237.

Greenwood, S., Ruiz-Benito, P., Martinez-Vilalta, J., Lloret, F., Kitzberger, T., Allen, C., Fensham, R., Laughlin, D., Kattge, J., Bönisch, G., Kraft, N., Jump, A., 2017. Tree mortality across biomes is promoted by drought intensity, lower wood density and higher specific leaf area. Ecol. Lett. 20, 539–553.

Hacket-Pain, A., Ascoli, D., Vacchiano, G., Biondi, F., Cavin, L., Conedera, M., Drobyshev, I., Dorado Liñán, I., Friend, A., Grabner, M., Hartl, C., Kreyling, J., Lebourgeois, F., Levanic, T., Menzel, A., van der Maaten, E., van der Maaten-Theunissen, M., Muffler, L., Motta, R., Zang, C., 2018. Climatically controlled reproduction drives inter-annual growth variability in a temperate tree species. Ecol. Lett. 21, 1833–1844.

Hacket-Pain, A., Cavin, L., Friend, A., Jump, A., 2016. Consistent limitation of growth by high temperature and low precipitation from range core to southern edge of European beech indicates widespread vulnerability to changing climate. Eur. J. For. Res. 135, 897–909.

Harris, I., Osborn, T.J., Jones, P., Lister, D., 2020. Version 4 of the CRU TS monthly high-resolution gridded multivariate climate dataset. Sci. Data 7, 109.

Hartmann, H., Moura, C.F., Anderegg, W.R.L., Ruehr, N.K., Salmon, Y., Allen, C.D., Arndt, S.K., Breshears, D.D., Davi, H., Galbraith, D., Ruthrof, K.X., Wunder, J., Adams, H.D., Bloemen, J., Cailleret, M., Cobb, R., Gessler, A., Grams, T.E.E., Jansen, S., Kautz, M., Lloret, F., O'Brien, M., 2018. Research frontiers for improving our understanding of drought- induced tree and forest mortality. New Phytol. 218, 15–28.

Hacket-Pain, A., Friend, A., 2017. Increased growth and reduced summer drought limitation at the southern limit of *Fagus sylvatica* L., despite regionally warmer and drier conditions. Dendrochronologia 44, 22–30.

Hammond, W.M., Williams, A.P., Abatzoglou, J.T., Adams, H.D., Klein, T., López, R., Sáenz-Romero, C., Hartmann, H., Breshears, D.D., Allen, C.D., 2022. Global field observations of tree die-off reveal hotter-drought fingerprint for Earth's forests. Nat. Commun. 13, 1761.

Herbette, S., Charrier, O., Cochard, H., Barigah, T.S., 2021. Delayed effect of drought on xylem vulnerability to embolism in *Fagus sylvatica*. Can. J. For. Res. 51, 622–626.

Holmes, 1983. Computer-assisted quality control in tree-ring dating and measurement. Tree Ring Bull. 43, 69–78.

IPCC, 2021. Climate Change 2021: the Physical Science Basis. Contribution of Working Group I to the Sixth Assessment Report of the Intergovernmental Panel on Climate Change. Cambridge University Press.

Jump, A.S., Hunt, J.M., Peñuelas, J., 2006. Rapid climate change-related growth decline at the southern range edge of *Fagus sylvatica*. Glob. Chang. Biol. 12, 2163–2174.

Kabeya, D., Inagaki, Y., Noguchi, K., Han, Q., 2017. Growth rate reduction causes a decline in the annual incremental trunk growth in masting *Fagus crenata* trees. Tree Physiol. 37, 1444–1452.

Karger, D.N., Conrad, O., Böhner, J., Kawohl, T., Kreft, H., Soria-Auza, R.W., Zimmermann, N.E., Linder, P., Kessler, M., 2017. Climatologies at high resolution for the Earth land surface areas. Sci. Data 4, 170122.

Karger, D.N., Conrad, O., Böhner, J., Kawohl, T., Kreft, H., Soria-Auza, R.W., Zimmermann, N.E., Linder, H.P., Kessler, M., 2018. Data from: Climatologies at High Resolution for the Earth's Land Surface Areas. https://doi.org/10.5061/dryad.kd1d4.

Klesse, S., von Arx, G., Gossner, M.M., Hug, C., Rigling, A., Queloz, V., 2021. Amplifying feedback loop between growth and wood anatomical characteristics of *Fraxinus excelsior* explains size-related susceptibility to ash dieback. Tree Physiol. 41, 683–696.

Larysch, E., Stangler, D.F., Nazari, M., Seifert, T., Kahle, H.P., 2021. Xylem phenology and growth response of European beech, silver fir and scots pine along an elevational gradient during the extreme drought year 2018. Forests 12, 75.

Leuschner, C., 2020. Drought response of European beech (*Fagus sylvatica* L.) —a review. Perspect. Plant Ecol. Evol. Syst. 47, 125576.

Martínez del Castillo, E., Longares, L.A., Gričar, J., Prislan, P., Gil-Pelegrín, E., Čufar, K., De Luis, M., 2016. Living on the edge: contrasted wood-formation dynamics in *Fagus sylvatica* and *Pinus sylvestris* under Mediterranean conditions. Front. Plant Sci. 7, 370.

Martínez del Castillo, E., Longares, L., Serrano-Notivoli, R., Sass-Klaassen, U., De Luis, M., 2019. Spatial patterns of climate–growth relationships across species distribution as a forest management tool in Moncayo Natural Park (Spain). Eur. J. For. Res. 138, 299–312.

Martínez del Castillo, E., Prislan, P., Gricar, J., Gryc, V., Merela, M., Giagli, K., De Luis, M., Vavrčík, H., Cufar, K., 2018. Challenges for growth of beech and co-occurring conifers in a changing climate context. Dendrochronologia 52, 1–10.

Martínez del Castillo, E., Zang, C.S., Buras, A., et al., 2022. Climate-change-driven growth decline of European beech forests. Commun. Biol. 5, 163.

Moser, L., Fonti, P., Büntgen, U., Esper, J., Luterbacher, J., Franzen, J., Frank, D., 2010. Timing and duration of European larch growing season along altitudinal gradients in the Swiss Alps. Tree Physiol. 30, 225–233.

Oberhuber, W., Swidrak, I., Pirkebner, D., Gruber, A., 2011. Temporal dynamics of nonstructural carbohydrates and xylem growth in *Pinus sylvestris* exposed to drought. Can. J. For. Res. 41, 1590–1597.

Oksanen J., Blanchet F.G., Friendly M., Kindt R., Legendre P., McGlinn D., Minchin P.R., O'Hara R.B., Simpson G.L., Solymos P., Stevens M.H.H., Szoecs E., Wagner H. (2020). vegan: Community ecology package. R package Version 2.5-7. https://CRAN.R-project.org/package=vegan.

Oladi, R., Bräuning, A., Pourtahmasi, K., 2014. Plastic" and "static" behavior of vessel-anatomical features in Oriental beech (*Fagus orientalis* Lipsky) in view of xylem hydraulic conductivity. Trees 28, 493–502.

Olano, J.M., Eugenio, M., García-Cervigón, A.I., Folch, M., Rozas, V., 2012. Quantitative tracheid anatomy reveals a complex environmental control of wood structure in continental mediterranean climate. Int. J. Plant Sci. 173, 137–149.

Olano, J.M., García-Cervigón, A.I., Sangüesa-Barreda, G., Rozas, V., Muñoz-Garachana, D., García-Hidalgo, M., García-Pedrero, A., 2021. Satellite data and machine learning reveal the incidence of late frost defoliations on Iberian beech forests. Ecol. Appl. 31, e02288.

Olson, M.E., Anfodillo, T., Gleason, S.M., McCulloh, K.A., 2021. Tip-to-base xylem conduit widening as an adaptation: causes, consequences, and empirical priorities. New Phytol. 229, 1877–1893.

Pérez-De-Lis, G., García-González, I., Rozas, V., Olano, J.M., 2016. Feedbacks between earlywood anatomy and non-structural carbohydrates affect spring phenology and wood production in ring-porous oaks. Biogeosciences 13, 5499–5510.

Peters, R., Steppe, K., Cuny, H., Pauw, D., Frank, D., Schaub, M., Rathgeber, C., Cabon, A., Fonti, P., 2020. Turgor - a limiting factor for radial growth in mature conifers along an elevational gradient. New Phytol. 229, 213–229.

Pfenninger M., Reuss F., Kiebler A., Schönnenbeck P., Caliendo C., Gerber S., Cocchiararo B., Reuter S., Blüthgen N., Mody K., Mishra B., Bálint M., Thines M., Feldmeyer B. (2021) Genomic basis for drought resistance in European beech forests threatened by climate change. Elife: 10:e65532.

Piovesan, G., Biondi, F., Filippo, A.D., Alessandrini, A., Maugeri, M., 2008. Drought-driven growth reduction in old beech (*Fagus sylvatica* L) forests of the central Apennines. Italy Glob. Chang. Biol. 6, 1265–1281.

Pluess, A.R., Weber, P., 2012. Drought-adaptation potential in *Fagus sylvatica*: linking moisture availability with genetic diversity and dendrochronology. PLoS One 7, e33636.

Postolache, D., Oddou-Muratorio, S., Vajana, E., Bagnoli, F., Guichoux, E., Hampe, A., Le Provost, G., Lesur, I., Popescu, F., Scotti, I., Piotti, A., Vendramin, G.G., 2021. Genetic signatures of divergent selection in European beech (*Fagus sylvatica* L.) are associated with the variation in temperature and precipitation across its distribution range. Mol. Ecol. 20, 5029–5047.

Pourtahmasi, K., Lotfiomran, N., Bräuning, A., Parsapajouh, D., 2011. Tree-ring width and vessel characteristics of oriental beech (*Fagus orientalis*) along an altitudinal gradient in the caspian forests, northern Iran. IAWA J. 32, 461–473.

Prislan, P., Gričar, J., Čufar, K., de Luis, M., Merela, M., Rossi, S., 2019. Growing season and radial growth predicted for *Fagus sylvatica* under climate change. Clim. Chang. 153, 181–197.

Prislan, P., Gričar, J., de Luis, M., Smith, K.T., Čufar, K., 2013. Phenological variation in xylem and phloem formation in *Fagus sylvatica* from two contrasting sites. Agric. For. Meteorol. 180, 142–151.

Prislan, P., K Čufar, K., De Luis, M., Gričar, J., 2018. Precipitation is not limiting for xylem formation dynamics and vessel development in European beech from two temperate forest sites. Tree Physiol. 38, 186–197.

R Core Team, 2020. R: A language and Environment For Statistical Computing. R Foundation for Statistical Computing. URL. https://www.R-project.org/.

Rathgeber, C., Cuny, H., Fonti, P., 2016. Biological basis of tree-ring formation: a crash course. Front. Plant Sci. 7.

Rever, C.P.O., Rammig, A., Brouwers, N., Langerwisch, F., 2015. Forest resilience, tipping points and global change processes. J. Ecol. 103, 1–4.

Rossi, S., Deslauriers, A., Gričar, J., Seo, J.W., Rathgeber, C.B.K., Anfodillo, T., Morin, H., Levanic, T., Oven, P., Jalkanen, R., 2008. Critical temperatures for xylogenesis in conifers of cold climates. Glob. Ecol. Biogeogr. 17, 696–707.

Rozas, V., Camarero, J.J., Sangüesa-Barreda, G., Souto, M., García-González, I., 2015. Summer drought and ENSO-related cloudiness distinctly drive *Fagus sylvatica* growth near the species rear-edge in northern Spain. Agric. For. Meteorol. 201, 153–164.

Sánchez, R., Gomez, C., Aulló-Maestro, I., Cañellas, I., Gea-Izquierdo, G., Montes, F., Ollero, H., Velazquez, J., Hernández, L., 2021. *Fagus sylvatica* L. peripheral populations in the mediterranean Iberian peninsula: climatic or anthropic relicts? Ecosystems 24. https://doi.org/10.1007/s10021-020-00513-8.

Sánchez-Salguero, R., Camarero, J.J., Gutiérrez, E., González-Rouco, F., Gazol, A., Sangüesa-Barreda, G., Andreu-Hayles, L., Linares, J.C., Seftigen, K., 2016. Assessing forest vulnerability to climate warming using a process-based model of tree growth: bad prospects for rear-edges. Glob. Chang. Biol. 23, 2705–2719.

Sangüesa-Barreda, G., Di Filippo, A., Piovesan, G., Rozas, V., Di Fiore, L., García-Hidalgo, M., García-Cervigón, A.I., Muñoz-Garachana, D., Baliva, M., Olano, J.M., 2021. Warmer springs have increased the frequency and extension of late-frost defoliations in southern European beech forests. Sci. Total Environ. 775, 145860.

Sass, U., Eckstein, D., 1995. The variability of vessel size in beech (*Fagus sylvatica* L.) and its ecophysiological interpretation. Trees 9, 247–252.

Serra-Maluquer, X., Gazol, A., Sangüesa-Barreda, G., Sánchez-Salguero, A., Rozas, V., Colangelo, M., Gutiérrez, E., Camarero, J.J., 2019. Geographically structured growth decline of rear-edge Iberian *Fagus sylvatica* forests after the 1980s shift toward a warmer climate. Ecosystems 22, 1325–1337.

Sperry, J., Meinzer, F., McCulloh, K., 2008. Safety and efficiency conflicts in hydraulic architecture: scaling from tissues to trees. Plant Cell. Environ. 31, 632–645.

Spinoni, J., Vogt, J.V., Naumann, G., Barbosa, P., Dosio, A., 2018. Will drought events become more frequent and severe in Europe? Int. J. Clim. 38, 1718–1736.

Steppe, K., Sterck, F., Deslauriers, A., 2015. Diel growth dynamics in tree stems: linking anatomy and ecophysiology. Trends Plant Sci. 20, 335–343.

von Arx, G., Arzac, A., Fonti, P., Frank, D., Zweifel, R., Rigling, A., Galiano, L., Gessler, A., Olano, J.M., 2017. Responses of sapwood ray parenchyma and non-structural carbohydrates (NSC) of *Pinus sylvestris* to drought and long-term irrigation. Funct. Ecol. 31, 1371–1382.

von Arx, G., Dietz, H., 2005. Aautomated image analysis of annual rings in the roots of perennial forbs. Int. J. Plant Sci. 166, 723–732.

Wigley, T.M.L., Briffa, K.R., Jones, P.D., 1984. On the average value of correlated time series, with applications in dendroclimatology and hydrometeorology. J. Clim. Appl. Meteorol. 201–213.

Zimmermann, J., Link, R.M., Hauck, M., Leuschner, C., Schuldt, B., 2021. 60-year record of stem xylem anatomy and related hydraulic modification under increased summer drought in ring- and diffuse-porous temperate broad-leaved tree species. Trees 35, 919–937.